ATP-EMTP Investigation of Adaptive Distance Protection for Transmissions Lines with Series Compensation

Piotr Mazniewski
Wroclaw University of Technology
Wroclaw, Poland
piotr.mazniewski@pwr.wroc.pl

Jan Izykowski
Wroclaw University of Technology
Wroclaw, Poland
jan.izykowski@pwr.wroc.pl

Abstract—**In this paper results of investigation of a new distance protection principle for a transmission line compensated with 3-phase capacitor banks installed at mid-line of the line is presented. The delivered distance protection algorithm applies two measurement procedures designated for determining fault loop impedance under faults in front of and behind the compensating bank, respectively. Presence of the resistance at fault is compensated for in both measurement procedures. The algorithm has been tested and evaluated with use of the fault data obtained from versatile ATP-EMTP simulations of faults in the test power network containing the 400-kV, 300-km series compensated transmission line. The sample results of the evaluation are reported and discussed.**

Keywords ***power transmission line; series compensation; fault simulation; ATP-EMTP; digital measurement; distance protective relay***

I. INTRODUCTION

Increased transmittable power, improved power system stability, reduced transmission losses, enhanced voltage control and flexible power flow control are the reasons behind installing Series Capacitors (SCs) on long transmission lines [2]. The environmental concerns stand for that too.

Both, capacitors of fixed value (FSC – Fixed Series Capacitors) and of controlled value (TCSC – Thyristor Controlled Series Capacitors) are installed in transmission lines. This paper deals with distance protection issues for a line compensated with a three-phase bank of fixed series capacitors (SCs) installed at mid-line (Fig. 1). SCs are equipped with their overvoltage protection devices: typically Metal Oxide Varistors (MOVs). Each MOV is in turn protected from overheating with the aid of the thermal protection (TP), which eventually sparks the respective Air-Gap, in order to by-pass its MOV.

The compensating bank when installed in a line, creates, however, certain problems for its protective relays and fault locators. If a series compensated line suffers a fault behind the SCs&MOVs, as seen from the relaying point (fault F_B in Fig. 1), a fault loop impedance measured by a distance relay contains, depending on a type of fault, one (for single phase faults) or even two (for inter–phase faults) SC&MOV units.

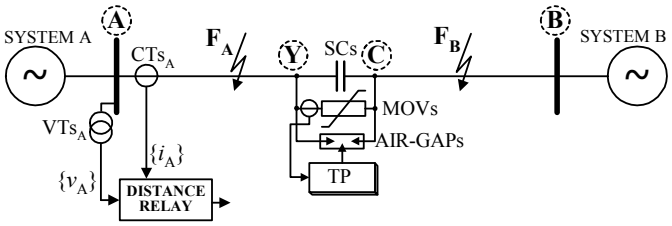

Figure 1. Schematic diagram of series compensated line for considering distance protection: F_A – fault in front of SCs&MOVs, F_B – fault behind SCs&MOVs.

Operating conditions of protective distance relays for series compensated lines become unfavorable and include such phenomena as voltage and/or current inversion, sub-harmonic oscillations, high frequency oscillations due to MOVs [2]. The most important singularity of a series compensated line as the object to be protected, lays, however, in the fact that the positive-sequence impedance measured by a traditional distance relay is no longer an indicator of the distance to a fault. The SC and its MOV affect both, the steady state and transient conditions of the distance relay measurements.

The aforementioned problems with protective relaying for series compensated lines are being extensively explored as a series of studies performed in [1], [3], [5]–[7], [9], [11], [14], [17]. Protection of networks with series compensated lines is considered as one of the most difficult tasks. However, there is still much room for developing efficient protective relaying for such networks. The approach presented in this paper is one of the attempts for accomplishing that.

II. MEASUREMENT OF FAULT LOOP IMPEDANCE FOR SERIES COMPENSATED LINE

Two distinctive hypothetical places of faults (F_A and F_B) are indicated in Fig. 1. In the case of the fault F_A (fault in front of the compensating bank) the measurement of fault loop impedance, performed by a distance relay from the substation A (Fig. 2), is basically analogous as for the traditional uncompensated line. In this case a fault resistance influences the measured fault loop impedance $\underline{Z}_{A\_p}$, as shown in Fig. 2. This impedance consists of the following two components:

- $d\underline{Z}_{1L}$ – positive-sequence impedance of the line section between the relaying point A and the fault point F_A (d denotes the per unit distance between these points),
- $\underline{R}_F^{\#}$ – complex impedance which represents the fault path resistance seen from the relaying point.

Fault loop impedance measurement for the case of the fault F_B (fault behind the compensating bank), performed by a distance relay from the substation A (Fig. 3), differs from the case of the fault F_A. In this case the fault loop impedance ($\underline{Z}_{A\_p}$) consists of the following three components:

- $d\underline{Z}_{1L}$ – positive-sequence impedance of the line section between the relaying point A and the fault point F_B,
- $\underline{R}_F^{\#}$ – complex impedance which represents the fault path resistance seen from the relaying point,
- ($R_{SC\&MOV}$–j$X_{SC\&MOV}$) – impedance of the R–C character, which represents presence of the compensating bank in the fault loop.

Note that in both Figs. 2 and 3, the complex impedance $\underline{R}_F^{\#}$ is drawn as not the pure resistance but twisted clockwise, i.e. by a certain angle from the range $[0 \div (-90^o)]$. However, it can remain untwisted (if there is no pre-fault power flow at all) or twisted counter-clockwise by a certain angle from the range $[0 \div 90^o]$.

Impedance which represents the compensating bank in the fault loop (Fig. 3) is not fixed, but depends on the current flowing through the bank [14].

Presence of the compensating bank in the fault loop substantially influences the fault loop impedance measurement. As a result of that, certain shortening of the distance protection reach for the first zone may happen, if special countermeasures are not undertaken. The voltage drop on the compensating device can be estimated with processing the current supplying the distance relay. Such effective procedure of estimation of this voltage drop was introduced in [15]. Presence of the compensating bank in the fault loop can be also reflected with use of the fundamental frequency equivalent principle delivered in [14].

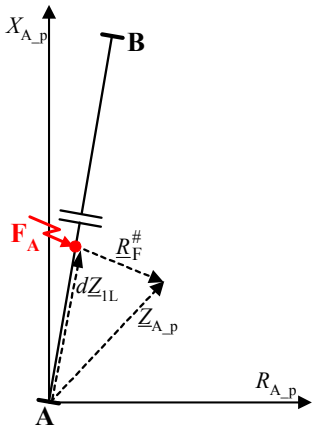

Figure 2. Measurement of fault loop impedance for the case of fault F_A occurring in front of SCs&MOVs.

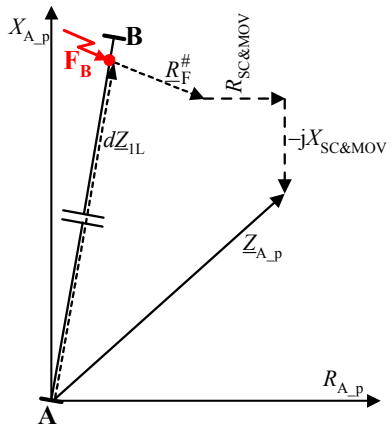

Figure 3. Measurement of fault loop impedance for the case of fault F_B occurring behind SCs&MOVs.

In order to counteract the negative influence of presence of the compensating bank in the fault loop (for faults occurring behind the bank) the position of the fault with respect to the bank (in terms whether occurred in front, or behind it), has to be recognized. This is so since the compensation for the compensating bank has to be applied only for faults occurring behind the compensating bank. In this way one concludes that two fault loop impedance measurement procedures have to be applied to adapt the distance protection for application to series compensated line. These two measurement procedures have to be supplemented with the algorithm for recognition of the position of a fault with respect to the compensating bank. The issue of such recognition algorithm is not addressed in this paper.

The other unfavorable conditions for operation of distance protective relays are related to the reactance effect [16] under resistive faults. Presence of resistance at a fault path results in falsifying the fault loop impedance measurement. As a result of that it could be impossible to make a proper and selective decision. One can distinguish two cases of wrong decisions reached by the distance protection relay due to the reactance effect:

- fault in the 1st zone – relay blocking,
- fault outside of the 1st zone – inadvertent relay operation.

In order to avoid both types of inappropriate operations of a distance protection for transmission lines with the series compensation, use of adaptation measures is proposed. The presented further adaptive distance protection is based on the fault location principle. Both applied measurement procedures for the fault loop impedance, which are relevant for faults in front of and behind the compensating bank (faults: F_A and F_B), undergo the similar principle of adaptation.

III. Adaptive Distance Protection

Fault loop impedance for the procedure F_A (for faults in front of SCs&MOVs) is proposed to be determined as:

$$\underline{Z}_{A\_p\_adapt}^{FA} = d_{FA} \cdot \underline{Z}_{1L} \tag{1}$$

where:
d_{FA} − the distance to the fault [p.u] from the relaying point A up to the fault F_A,
$\underline{Z}_{1L}$ – the line impedance for the positive-sequence.

It is considered that the distance d_{FA} from (1) is determined according to the algorithm introduced by A. Wiszniewski, for which the details can be found in [7], [8], [16]. The cited algorithm applies the measurement of three-phase current and voltage from one end of the line and assumes that the fault current distribution factors for the positive- and negative-sequence are real numbers.

Fault loop impedance for the procedure F_B (for faults behind SCs&MOVs) is proposed to be determined as:

$$\underline{Z}^{FB}_{A\_p\_adapt} = d_{FB} \cdot \underline{Z}_{1L} \tag{2}$$

where:
d_{FB} − the distance to the fault [p.u] from the relaying point A up to the fault F_B.

The distance to the fault (d_{FB}) involved in (2) is determined:

$$d_{FB} = m_{[p.u]} \cdot \left(1 - p_{[p.u]}\right) + p_{[p.u]} \tag{3}$$

where:
m – the 'new' distance to fault [p.u], from the point C up to the fault F_B (Figs. 1 and 4), related to the length of the line section C–B,
p − the distance between the bus A and the point at which the compensating bank is installed [p.u.].

In the procedure F_B (for faults behind the compensating bank) the measurement of the distance 'm' was derived based on the models from Fig. 4. The fault loop model (4), which combines the models for individual symmetrical components, has been stated. In these models (Fig. 4a–d) the analytical transfer of voltage and current signals from the bus A up to the point C (Fig. 1) is acomplished. Making such analytical transfer involves estimation of the voltage drop across the compensating bank, as shown in the references [7], [8], [15].

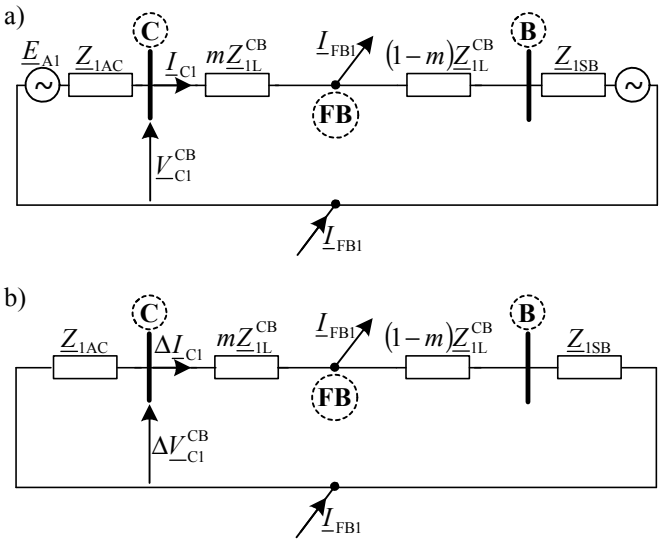

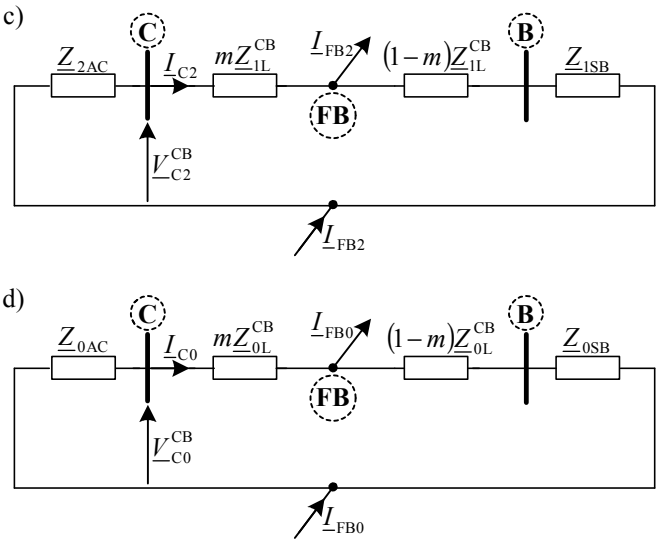

Figure 4. Circuit diagram of a single line for symmetrical components after analytic transfer signals for respective sequences: a) positive-, b) incremental-positive-, c) negative-, c) zero-.

Based on the diagrams of Fig. 4 the following generalized fault loop model can be stated:

$$\underline{V}^{CB}_{C\_p} - m\underline{Z}^{CB}_{1L}\underline{I}^{CB}_{C\_p} - \frac{R_F}{\underline{K}_1 m + \underline{L}_1}\left(\underline{a}_{F1}\Delta\underline{I}_{C1}\underline{M}_1 + \underline{a}_{F2}\underline{I}_{C2}\underline{M}_2\right) \tag{4}$$

where:
$\underline{V}^{CB}_{C\_p} = \underline{a}_1\underline{V}^{CB}_{C1} + \underline{a}_2\underline{V}^{CB}_{C2} + \underline{a}_0\underline{V}^{CB}_{C0}$ – fault loop voltage,
$\underline{V}^{CB}_{C1} = \left(\underline{V}_{AA1} - p\underline{Z}_{1L}\underline{I}_{AA1}\right) - \underline{V}_{SC/MOV\_1}$,
$\underline{V}^{CB}_{C2} = \left(\underline{V}_{AA2} - p\underline{Z}_{1L}\underline{I}_{AA2}\right) - \underline{V}_{SC/MOV\_2}$,
$\underline{V}^{CB}_{C0} = \left(\underline{V}_{AA0} - p\underline{Z}_{0L}\underline{I}_{AA0}\right) - \underline{V}_{SC/MOV\_0}$,
$\underline{V}_{SC/MOV\_i}$ – estimated voltage drop across the compensating bank for the ith symmetrical component [31, 93],
$\underline{I}^{CB}_{C\_p} = \underline{a}_1\underline{I}_{C1} + \underline{a}_2\underline{I}_{C2} + \underline{a}_0\underline{k}^{CB}_0\underline{I}_{C0} + \underline{a}_0\underline{k}^{CB}_{0m}\underline{I}_{C0\_paral}$ – fault loop current ($\underline{I}_{C1} = \underline{I}_{AA1}$, $\underline{I}_{C2} = \underline{I}_{AA2}$, $\underline{I}_{C0} = \underline{I}_{AA0}$,
$\underline{I}_{C0\_paral}$ – zero-sequence current from the healthy parallel line),
$\underline{Z}^{CB}_{C\_p} = \dfrac{\underline{V}^{CB}_{C\_p}}{\underline{I}^{CB}_{C\_p}}$ – fault loop impedance,
$\underline{k}^{CB}_0 = \dfrac{\underline{Z}^{CB}_{0L}}{\underline{Z}^{CB}_{1L}}$ – coefficient used for both the single- and double-circuit lines,
$\underline{k}^{CB}_{0m} = \dfrac{\underline{Z}^{CB}_{0m}}{\underline{Z}^{CB}_{1L}}$ – coefficient in the case of the double-circuit line,
$\underline{Z}_{1AC} = \dfrac{-\Delta\underline{V}_{C1}}{\Delta\underline{I}_{C1}}$ – equivalent impedance seen from the point C to the left side (the system A, the line section A–Y, the compensating bank) for the positive-sequence component,

$\underline{Z}_{2AC} = \dfrac{-\underline{V}_{C2}}{\underline{I}_{C2}}$ – as $\underline{Z}_{1AC}$, but for the negative-sequence,

$\Delta\underline{I}_{C1} = \underline{I}_{C1} - \underline{I}_{C1}^{pre}$, $\Delta\underline{V}_{C1} = \underline{V}_{C1} - \underline{V}_{C1}^{pre}$ – incremental positive-sequence quantities ('fault quantity' *minus* 'pre-fault quantity')

$\underline{K}_1 = -\underline{Z}_{1L}^{CB}$, $\underline{L}_1 = \underline{Z}_{1L}^{CB} + \underline{Z}_{1SB}$,

$\underline{M}_1 = \underline{Z}_{1AC} + \underline{Z}_{1L}^{CB} + \underline{Z}_{1SB}$, $\underline{M}_2 = \underline{Z}_{2AC} + \underline{Z}_{1L}^{CB} + \underline{Z}_{1SB}$,

$\underline{a}_{F1}$, $\underline{a}_{F2}$ – share coefficients, dependent on the fault type and assumed priority for using particular symmetrical components (Table I).

IV. Simulations and Tests Conducted With Use Of ATP-EMTP and MATLAB Programs

The presented subroutines of the fault loop impedance measurement have been tested and evaluated with the fault data obtained from versatile ATP-EMTP [4], [12] simulations of faults in the test power network. Basic parameters are gathered in Table II.

The test power network contains the 400 kV, 300 km transmission line, compensated with a three-phase bank of series capacitors installed at mid-line. The compensation rate of 70% was assumed. MOVs installed in parallel to series capacitors were modeled as nonlinear resistors defined with the analytical characteristic and its parameters as given in Table II. The thermal protection (TP in Fig. 1) preventing the MOV from overheating was modeled as the component integrating the accumulated energy. After exceeding the set threshold for energy, the sparking of the associated air-gap undergoes, and the MOV becomes shunted. It has been checked that for the considered application, i.e. for the high-speed protective relaying, the air-gap sparking does not take place prior to making the decision by the distance relay. Thus, the thermal protection does not influence a fault loop impedance measurement of the distance protection.

TABLE I. Alternative Sets of Shares Coefficients with Eliminating Zero–Sequence [7], [8]

Kind Fault	Set weighting coefficients with eliminating zero-sequence ($\underline{a}_{F0} = 0$)			
	Set I		Set II	
	$\underline{a}_{F1}$	$\underline{a}_{F2}$	$\underline{a}_{F1}$	$\underline{a}_{F2}$
L1– G	0	3	3	0
L2– G	0	$3\underline{a}$	$3\underline{a}^2$	0
L3– G	0	$3\underline{a}^2$	$3\underline{a}$	0
L1–L2	0	$1-\underline{a}$	$1-\underline{a}^2$	0
L2–L3	0	$\underline{a}-\underline{a}^2$	$\underline{a}^2-\underline{a}$	0
L3–L1	0	$\underline{a}^2-1$	$\underline{a}-1$	0
L1–L2– G	$1-\underline{a}^2$	$1-\underline{a}$	$1-\underline{a}^2$	$1-\underline{a}$
L2–L3– G	$\underline{a}^2-\underline{a}$	$\underline{a}-\underline{a}^2$	$\underline{a}^2-\underline{a}$	$\underline{a}-\underline{a}^2$
L3–L1– G	$\underline{a}-1$	$\underline{a}^2-1$	$1-\underline{a}^2$	0

TABLE II. Basic Parameters of the Test Transmission Network

Equivalent system at terminal A (φ=0°)	$\underline{Z}_{1SA}$	(0.656+j7.5) Ω
	$\underline{Z}_{0SA}$	(1.167+j11.25) Ω
Equivalent system at terminal B (φ= –15°)	$\underline{Z}_{1SB}$	(1.31+j15) Ω
	$\underline{Z}_{0SB}$	(2.33+j26.6) Ω
Line AB	$\underline{Z}'_{1L}$	(0.028+j0.315) Ω/km
	$\underline{Z}'_{0L}$	(0.275+j1.027) Ω/km
	C'_{1L}	13.0 nF/km
	C'_{0L}	8.5 nF/km
Series compensation	Series capacitors	0.70 X_{1L}
	Position of the compensating bank	0.5 p.u.
MOV characteristic: $i_{MOV} = P\left(\dfrac{V_V}{V_{REF}}\right)^q$	P	1 kA
	V_{REF}	150 kV
	q	23
Line length		300 km
System voltage		400 kV

The model includes the Capacitive Voltage Transformers (CVTs) and the Current Transformers (CTs). The analog filters with 350 Hz cut-off frequency were also included. The sampling frequency of 1000 Hz was applied.

The following parameters have been altered in the evaluation study:

- distance to fault – 18 values: 10, 30, 40, 45, 50, 60, 90, 120, 149, 151, 180, 210, 240, 250, 255, 260, 270, 290 [km],
- fault resistance:
  for faults L–G and L–L–G – 5 values: 0.1, 5, 10, 25, 50 [Ω],
  for faults L–L, L–L–L (L–L–L–G) – 5 values: 0.1, 0.5, 1, 2, 5 [Ω],
- point on the wave at which the fault is applied – 2 cases: the angle 0° (at zero crossing) and 90° (at maximum),
- impedance system: – 4 cases: (strong–strong, strong–week, week–strong, week–week),
- angle of EMFs at the end A was set as φ=0° (the cosine wave with zero phase shift in the phase 'L1'), while for the end B – 4 cases: –20°, –15°, 15°, 20°.

The presented algorithms for adaptive distance protection (equations (1) and (2)) has been reflected in MATLAB environment [10].

Example 1 (Fig. 5), the results are presented for a single phase to ground fault (L1–G) in front of SC&MOV for the following conditions: fault position − d = 0.2 p.u, fault resistance − R_F = 25 Ω, the direction of pre-fault active power flow from station A to B.

Example 2 (Fig. 6), the results are presented for a single phase to ground fault (L1–G) behind SC&MOV for the following conditions: fault position − d = 0.7 p.u, fault resistance − R_F = 25 Ω, the direction of pre-fault active power flow from station A to B.

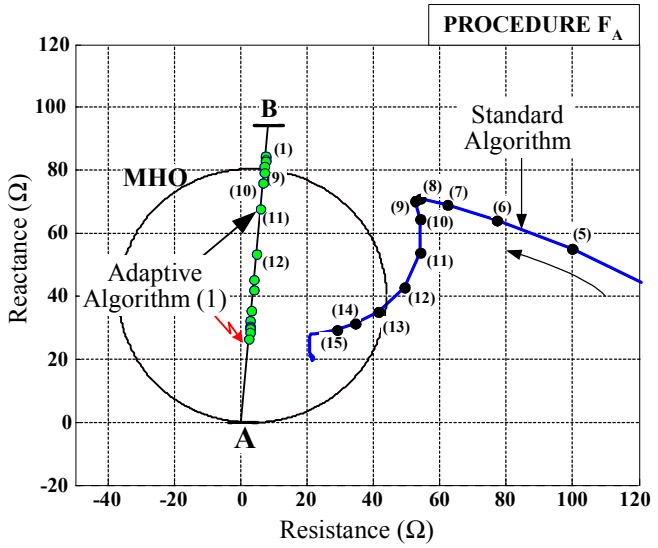

Figure 5. Example 1 (fault in front of SCs/MOVs) – the trajectories of fault loop impedance for the procedure F_A.

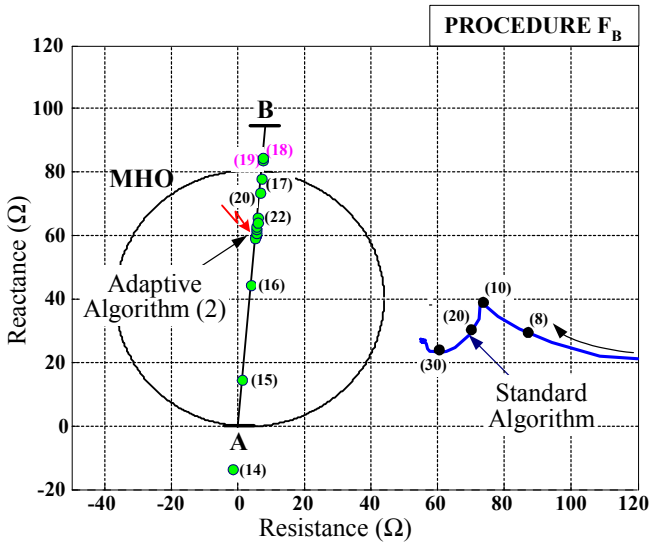

Figure 6. Example 2 (fault behind of SCs/MOVs) – the trajectories of fault loop impedance for the procedure F_B.

Figs. 5 and 6 present the trajectories of fault loop impedance measured by a distance relay when applying three different measurement algorithms: the standard – according to the classical distance protection principle, adaptive (1) – according to the formula (1), adaptive (2) – according to the formula (2). Numbers in parentheses (*n*) denote the number of samples from the fault inception instant. MHO characteristics of the first zone distance protection, set at 85% of the line length are shown Figs. 5 and 6 as well.

As shown in Fig. 5 (Example 1) the trajectories for both kinds of fault loop impedance measurements encroach the MHO characteristic. However, the encroachment in the case of the adaptive algorithm (1) is faster than for the standard algorithm.

In turn, for the Example 2 (Fig. 6) the trajectory of the fault loop impedance measured according to the standard algorithm does not encroach the MHO characteristic at all, which means that there will be a missing operation for this fault (fault inside the first protective zone). This is a result of the combined effect of both inclusion of the SC&MOV in the fault loop and presence of the resistance at fault. In contrast, the trajectory of the fault loop impedance measured according to the adaptive algorithm (2) encroaches the MHO characteristic and thus there will be a needed tripping. This is worth to observe that the trajectory of the impedance measured according to the adaptive algorithm (2) encroaches the MHO characteristic for a certain number of samples and then goes out of this characteristic for two samples (at 18 and 19 ms of the fault time) and again places inside the characteristic. This is not danger for making the correct decision since it was taken that the decision is reached on the base of the placement of 5 consecutive samples of the fault loop impedance inside the characteristic.

Table III presents the results for single-phase to ground faults (L1–G) involving fault resistance equal to 25 Ω, for the direction of the pre-fault active power flow from the station A towards B. The table shows the results of different algorithms operation, with marking: Y – if there is a tripping (in such cases additionally the tripping time is provided), N – if there is no tripping. In Table III, the distance to fault $d = 0.5^-$ p.u. denotes that a fault occurred at a distance of 0.5 p.u., but from the left side of the compensating bank (Fig. 1 – point Y). Conversely, the distance to fault $d = 0.5^+$ denotes that a fault occurred at a distance of 0.5 p.u., but from the right side of the compensating bank (Figs. 1 and 4 – point C). With the sign * it is marked that the behavior of a given algorithm is not of our interest.

Based on the results obtained from Table III it can be concluded that the introduction of two measurement procedures improved the efficiency of distance protection for the single-phase to ground faults considered here. As can be seen from the presented results, the introduction of adaptive algorithms for distance protection has improved its operation by reducing the fault detection time and increasing confidence in the reached decisions by eliminating the missing operations.

TABLE III. COMPARISON OF THE PERFORMANCE OF THE ADAPTIVE AND STANDARD ALGORITHMS

d_{real} [p.u]	**Procedure F_A**				**Procedure F_B**			
	Standard Algorithm		*Adaptive Algorithm (1)*		*Standard Algorithm*		*Adaptive Algorithm (2)*	
	TRIP	Time [ms]	TRIP	Time [ms]	TRIP	Time [ms]	TRIP	Time [ms]
0.1	Y	11	Y	6	*	*	*	*
0.2	Y	12	Y	9	*	*	*	*
0.3	Y	13	Y	10	*	*	*	*
0.4	Y	15	Y	11	*	*	*	*
0.5^-	Y	16	Y	12	*	*	*	*
0.5^+	*	*	*	*	N	–	Y	15
0.6	*	*	*	*	N	–	Y	15
0.7	*	*	*	*	N	–	Y	21
0.8	*	*	*	*	N	–	Y	22
0.85	*	*	*	*	N	–	Y	22
0.9	*	*	*	*	N	–	N	–

As can be seen in the Table III, application of the standard algorithm for the fault loop measurement results in shortening of the relay reach up to 0.5⁻ p.u. This means that for all faults occurring behind the compensating bank there will be no tripping for the relay first zone.

V. CONCLUSIONS

This paper deals with the problems of distance protection for transmission lines with series compensation. The analysis shows that using a traditional distance protection to the line with installed capacitor compensating banks results in shortening of the distance relay first zone.

In order to adapt the distance relay for application to series compensated line, the use of two fault loop impedance measurement procedures is considered. These procedures have to be applied together with the selection of the faulted line section. This selection, applied for deciding whether a fault occurred in front of or behind the compensating bank, is the subject of further work of the authors of this paper.

It can be concluded from the evaluation performed with utilization of the simulation fault data that the application of the proposed measuring algorithms resulted in selective and fast identification of faults. The presented results show that it is possible to offset the negative impact of the reactance effect relevant for resistive faults. Also reduction of time needed to make the correct decision has been obtained.

Tests results allow to state that the developed procedures for fault loop impedance measurement are able to enhance firmly dependability of the distance relay, which is nowadays of very high importance.

REFERENCES

[1] B. Bachmann, D. Novosel, D. Hart, Y. Hu and M. M. Saha, "Application of artificial neural networks for series compensated line protection," International Conference on Intelligent Systems Applications to Power Systems, Orlando, FL, pp. 68–73, Jan. 28–Feb. 02, 1996.

[2] CICGRE SC-34 WG-04, "Application guide on protection of complex transmission network configurations," CIGRE materials, August 1990.

[3] P. K. Dash, S. R. Samantaray and G. Panda, "Fault classification and section identification of an advanced series-compensated transmission line using support vector machine," IEEE Trans. on Power Del., vol. 22, no. 1, pp. 67–73, Jan. 2007.

[4] H. W. Dommel, "Electro-Magnetic Transients Program," BPA, Portland, Oregon, 1986.

[5] A. A. Girigis, A. A. Sallam and A. K. El-Din, "An adaptive protection scheme for advanced series compensated (ASC) transmission lines," IEEE Trans. on Power Del., vol. 13, no. 2, pp. 414–420, Apr. 1998.

[6] F. Ghassemi, J. Goodarzi and A. T. Johns, "Method for eliminating the effect of MOV operation on digital distance relays when used in series compensated lines," Universities Power Engineering Conference, Manchester, UK, Sept. 10–12, 1997 pp. 113–116.

[7] J. Izykowski, Impedance-based fault location algorithms", Publisher of Wroclaw University of Technology, 2001 –book in polish.

[8] J. Izykowski,"Fault location on power transmission lines", Oficyna Wydawnicza PWr, 2008 – polish book

[9] J. A. S. B. Jayasinghe, R. K. Aggarwal, A. T. Johns and Z. Q. Bo, "A novel non-unit protection for series compensated EHV transmission lines based on fault generated high frequency voltage signals," IEEE Trans. on Power Del., vol. 13, no. 2, pp. 405–413, Apr. 1998.

[10] MATLAB, High-performance numeric computation and visualization software. External interface guide, The Mathworks, Inc., January 1993.

[11] D. Novosel, A. Phadke, M. M. Saha and S. Lindahl, "Problems and solutions for microprocessor protection of series compensated lines," 6th International Conference on Developments in Power System Protection, Nottingham, UK, Conference Publication No. 434, IEE 1997, pp. 18–23, 25–27 March 1997.

[12] E. Rosolowski, "Computer methods of electromagnetic transient analysis", Publisher of Wroclaw University of Technology, 2009 – book in polish.

[13] E. Rosolowski, J. Izykowski and B. Kasztenny, "A new half – cycle adaptive phasor estimator immune to the decaying dc component for digital protective relaying," North America Power Systems (NAPS) Conference, University of Waterloo, Canada, October 23–24, 2000.

[14] E. Rosolowski, J. Izykowski, B. Kasztenny and M. M. Saha, "A new accurate fault algorithm for series compensated lines," IEEE Trans. on Power Del., vol. 14, no. 3, Jan. 1999, pp. 789–795.

[15] E. Rosolowski, J. Izykowski, B. Kasztenny and M. M. Saha, "First zone algorithm for protection of series compensated lines," IEEE Trans. on Power Del., vol. 16, no. 2, Apr. 2001, pp. 67–73.

[16] A. Wiszniewski, "Accurate fault impedance locating algorithm", IEE Proceedings – Part C, vol. 130, no. 6, 1983, pp. 311–315.

[17] Q. Y. Xuan, Y. H. Song, A. T. Johns, R. Morgan and D. Williams, "Performance of an adaptive protection scheme for series compensated EHV transmission systems using neural networks," Electric Power System Research, vol. 36, no. 1, Jan. 1996, pp. 57–66.